An Ultrathin Liquid Film Lubrication Theory—Calculation Method of Solvation Pressure and Its Application to the EHL Problem

Hiroshige Matsuoka
Graduate Student.

Takahisa Kato
Associate Professor.

Department of Mechanical Engineering,
The University of Tokyo
7-3-1 Hongo, Bunkyo-ku, Tokyo,
113, Japan

This paper describes a new method for calculating the solvation pressure that acts between solid surfaces when the surfaces approach each other to within a very small distance in a liquid medium. Solvation pressure is calculated by solving the transformed Ornstein-Zernike equation for hard-spheres in a two-phase system with Perram's method and using the Derjaguin approximation. Furthermore, the authors apply the new method to the elastohydrodynamic lubrication problem in which the film thickness is very small and solvation force and van der Waals force cannot be neglected. It will be shown that the calculation results agree well with experimental data. The results are then compared with two conventional solvation pressure models proposed so far, namely, Chan and Horn's model, and, Jang and Tichy's model. It is found that these two models neglect the elastic deformation of solid surface when obtaining the experimental parameter used in their models; thus they overestimate the solvation pressure resulting in the prediction of larger film thickness than the experiments.

1 Introduction

Machine elements are being downsized in recent years with the advance of micromachining technology. In accordance with this downsizing, the separation between surfaces that move relative to each other becomes smaller and smaller. For example, in the case of a hard disk drive system of a computer, the flying height of a magnetic head over a disk surface is approaching a few or a few tens of nanometers, and a system in which the head-disk interface is immersed in liquid lubricant instead of air has been considered (de Bruyne and Bogy, 1994; Ikeda and Tago, 1995). Therefore, knowledge concerning the characteristics of very thin lubricant films will be indispensable as the basis of key technologies in the near future (van Alsten and Granick, 1988, 1990; Granick, 1991; Granick and Hu, 1994; Granick et al., 1995; Peachey et al., 1991; Carson et al., 1992; Homola, 1991; Homola et al., 1989; Israelachvili et al., 1988; Georges et al., 1993(a), (b), 1995; Johnston et al., 1991; Guangteng and Spikes, 1994, 1995; Smeeth et al., 1995(a), (b); Spikes, 1995; Luo et al., 1995).

The authors developed a new apparatus which measures ultrathin fluid lubrication film thickness. As a result of the film thickness measurements using the apparatus, the authors observed discretization of the film thickness due to solvation force when it is less than about 10 nm (Matsuoka and Kato, 1996). Solvation force (often called structural force) is a unique force which acts between two solid surfaces when the two surfaces approach each other to very small distance in a liquid, and is schematically shown in Fig. 1. From the several past experimental studies (Homola et al., 1989; Horn and Israelachvili, 1981; Christenson, 1983) and theoretical studies, e.g., Monte Carlo simulation or molecular dynamics (Tarazona and Vicente, 1985; van Megen and Snook, 1979; Bitsanis et al., 1987), it is known that the solvation force has the following characteristics: (i) an oscillatory force which decays exponentially with surface separation, and (ii) the period of the oscillation with surface separation is roughly same as the diameter of intervening liquid molecule. The solvation force which has such characteristics as mentioned above is not negligible in the case of ultrathin film lubrication. A lubrication theory considering the solvation force is required in such a ultrathin film lubrication since the solid surface will deform elastically, not only from the viscous force but also from the solvation force. In this study, a new calculation method of solvation force per unit area between planes (we call the solvation force "solvation pressure" hereafter) is presented first, and then the solvation pressures are considered in EHL calculations and the calculated film thicknesses are compared with experiments.

There are several EHL theories for thin fluid film proposed by Tichy and coworkers, e.g., director model (Tichy, 1995(a)), surface layer model (Tichy, 1995(b)), porous media model (Tichy, 1995(c)) and exp-cos solvation pressure model (Jang and Tichy, 1995). The authors select the last model of them since others include unknown parameters which cannot be estimated easily. Another exp-cos solvation force model proposed by Chan and Horn (Chan and Horn, 1985) is also applicable to the EHL calculation. These two solvation pressure models are compared with the experiments and the calculation results of the present model.

2 Pressures Between Solid Walls Separated by Ultrathin Liquid Film

In conventional EHL theory, film thickness and pressure distribution are obtained by solving the Reynolds equation and elasticity equations simultaneously. The authors reported that the measured film thickness deviates from the conventional EHL theory and discussed the possibility that the deviation can be attributed to solvation force when the film thickness is of

Contributed by the Tribology Division of THE AMERICAN SOCIETY OF MECHANICAL ENGINEERS and presented at the ASME/STLE Joint Tribology Conference, San Francisco, Calif., October 13–17, 1996. Manuscript received by the Tribology Division January 25, 1996: revised manuscript received May 20, 1996. Paper No. 96-Trib-16. Associate Technical Editor: C. Cusano.

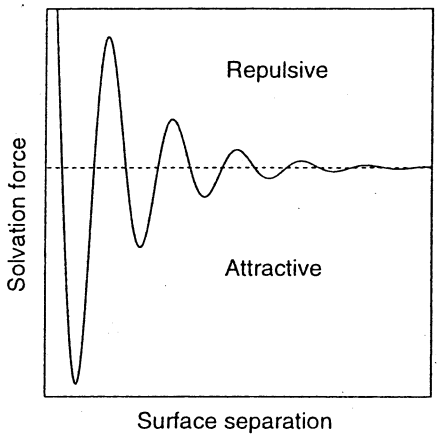

Fig. 1 Solvation force, showing oscillation and exponential decay schematically

the order of a few nanometers (Matsuoka and Kato, 1996). Hence, as described in the Introduction section, an EHL theory considering solvation pressure is necessary. Furthermore, in case of ultrathin film thickness (about a few nanometers), a pressure caused by the van der Waals force between solid surfaces (we call the pressure "van der Waals pressure") should be considered. We assume that the total pressure, p, is composed of three components, i.e., solvation pressure, p_s, van der Waals pressure, p_{vdW}, and conventional viscous pressure, p_h, namely,

$$p = p_s + p_{vdW} + p_h. \tag{1}$$

The total pressure, p, in expression (1) is calculated simultaneously with the elasticity equations as in conventional EHL theory. Calculation methods for these three pressure components are mentioned in the following sections.

3 Solvation Pressure

3.1 Basic Idea. First, we consider how the solvation force which has characteristics described in the Introduction section is generated. The structure of liquid between solid walls is shown in Fig. 2, in which circles denote molecules schematically. Considering density (number density) of liquid molecules between solid surfaces, the density under the condition shown in Fig. 2(a) is higher than that of Fig. 2(b). The periodic density change between solid surfaces in this manner with the increase in surface separation generates periodically changing force called solvation force (Tarazona and Vicente, 1985; Snook and van Megen, 1979). Therefore, the solvation force can be calculated by considering the density distribution between surfaces as a function of surface separation.

Now we consider a multiparticle system as shown in Fig. 3 and consider an interaction energy between particles. Taking notice of any one of the particles in the system, we introduce the radial distribution function, $g(r)$, where r denotes distance from center of the particle, by which the distribution of particles in the system is presented. Interaction energy between the first

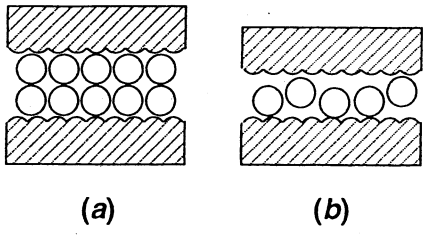

Fig. 2 Liquid molecules between solid walls. (a) dense; (b) dilute.

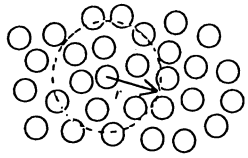

Fig. 3 One-phase system. The system is composed of one kind of many particles (diameter σ).

particle and another second particle with distance, r, is given approximately by using a linear theory (Henderson and Lozada-Cassou, 1986):

$$W^{s-s}(r) \approx -k_B T\{g(r) - 1\}, \tag{2}$$

where $s - s$ means interaction between a $s$phere and a $s$phere, k_B is the Boltzmann constant and T is the temperature in degrees Kelvin. Expression (2) is the energy caused by structure of multiparticle system (distribution of particles) as shown in Fig. 3, and we call it "solvation energy" or "structural energy." From the solvation energy written in expression (2), a net solvation force which acts between the two particles (spheres) with the distance r is given by

$$F^{s-s}(r) = -\frac{dW^{s-s}(r)}{dr}. \tag{3}$$

In order to convert a net force between spheres into a force between planes per unit area, namely, pressure, the Derjaguin approximation is often used. This approximation combines a net force between spheres and a energy between planes per unit area, and is written in

$$W^{p-p}(r) = \frac{F^{s-s}(r)}{2\pi R^{\text{eff}}} \tag{4}$$

where $p - p$ means interaction between a $p$lane and a $p$lane, and R^{eff} is an effective radius of curvature of interacting spheres. The Derjaguin approximation and rigorous expression of R^{eff} are described in detail by White (1983). Finally, the force between planes per unit area, F^{p-p}, namely, the solvation pressure, p_s, is obtained by the same relation as expression (3) and is given by

$$p_s = F^{p-p}(r) = -\frac{dW^{p-p}(r)}{dr} = \frac{1}{2\pi R^{\text{eff}}}\frac{d^2W^{s-s}(r)}{dr^2}$$

$$= -\frac{k_B T}{2\pi R^{\text{eff}}}\frac{d^2 g(r)}{dr^2}. \tag{5}$$

It is found that if the radial distribution function, $g(r)$, is obtained, then the solvation pressure can be calculated from expression (5). Therefore, the main problem is to obtain $g(r)$.

Direct calculation method such as Monte Carlo simulation and molecular dynamics (Bitsanis et al., 1987; Snook and van Megen, 1980, 1981; Alder et al., 1955) have been proposed in order to calculate the radial distribution function. The authors, however, do not use these methods because considerable calculation time is required, but take a method by means of a statistical approximation, in which $g(r)$ is given by an integral equation. In the present study $g(r)$ is calculated from the integral equation by supposing hard-sphere particles.

3.2 Example of Calculation of Radial Distribution Function in One-Phase System by Perram's Method. We start with calculation of the radial distribution function of a system composed of one kind of particles of diameter σ (we call the system "one-phase system") shown in Fig. 3. There are several equations for $g(r)$ proposed for this system, e.g., Born-Green-Yvon equation and convolution hypernetted chain equation (Throop and Bearman, 1965), but in this study, the authors

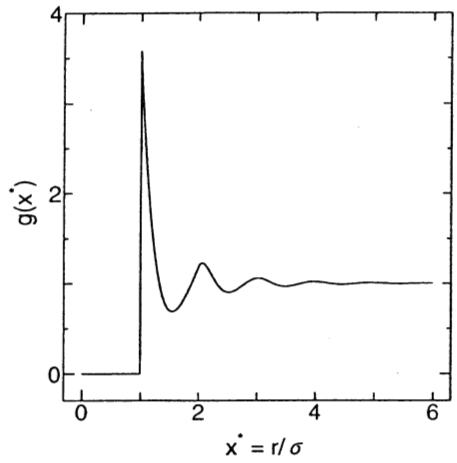

Fig. 4 Radial distribution function, $g(x^*)$, in one-phase system calculated by Perram's method. $N = 100$, $\rho^*\sigma^3 = 0.8$.

adopt the Ornstein-Zernike (OZ) equation, which agrees well with the results of Monte Carlo simulation and molecular dynamics (Ornstein and Zernike, 1914; Wertheim, 1963, 1964). The OZ equation for hard-spheres in a one-phase system is given by (Perram, 1975)

$$h^*(r) = c^*(r) + \rho^* \int h^*(|r - s|)c^*(s)ds,$$

$$h^*(r) = g(r) - 1, \tag{6}$$

where $h^*(r)$ is the indirect correlation function, $c^*(r)$ is the direct correlation function, and ρ^* is number density of particles when $r \to \infty$. Wertheim (Wertheim, 1963, 1964; Smith and Henderson, 1970) first solved Eq. (6) with respect to $g(r)$ explicitly by transforming Eq. (6) into the Percus-Yevick equation (Percus and Yevick, 1958). This analytical solution, however, is so complicated that it is not calculated easily. On the other hand, Perram proposed a numerical solution of the OZ equation (Perram, 1975). Perram's method (stepwise method) has several advantages, namely, (i) being easy to formulate, (ii) being able to calculate up to large r, (iii) requiring short calculation time compared with other numerical methods. Therefore, in this study, we obtain the radial distribution function by using Perram's method (stepwise method).

In order to use the Perram's method, the OZ equation (6) is transformed into the following equation,

$$\begin{cases} h^*(x^*) = -1, & \text{for} \quad x^* < 1 \\ x^*h^*(x^*) = -q'(x^*) + 12\eta^* & \\ \quad \times \displaystyle\int_0^1 (x^* - t)h^*(|x^* - t|)q(t)dt, & \text{for} \quad x^* \geq 1, \end{cases} \tag{7}$$

where

$$\begin{cases} x^* = r/\sigma \\ \eta^* = \pi\rho^*\sigma^3/6 \\ q'(x^*) = 0, \quad \text{for} \quad x^* \geq 1 \\ q'(x^*) = a_1x^* + a_2 \quad \text{for} \quad x^* < 1 \\ q(x^*) = 0, \quad \text{for} \quad x^* \geq 1 \\ q(x^*) = \dfrac{1}{2}a_1(x^{*2} - 1) + a_2(x^* - 1), \quad \text{for} \quad x^* < 1 \\ a_1 = \dfrac{2\eta^* + 1}{(\eta^* - 1)^2} \\ a_2 = \dfrac{-3\eta^*}{2(\eta^* - 1)^2} \end{cases} \tag{8}$$

Equation (7) is called the transformed Ornstein-Zernike equation. Eq. (7) is discretized to solve numerically by a computer. Putting $\theta(x^*) = x^*h^*(x^*)$, $\theta(x^*) = -x^*$ for $x^* < 1$ because $h^*(x^*) = -1$ in this region. Let us choose a suitable spacing δ, then we have $(N + 1)$ points in $0 \leq t \leq 1$, $0 \leq x^* \leq 1$, i.e., $0, \delta, 2\delta, \ldots, N\delta = 1.0$ at which $q_k = q(k\delta)$, $\theta_k = k\delta h(k\delta)$, and $g_k = g(k\delta)$ (k: integer). Performing the integration in Eq. (7) by the trapezoidal rule, namely,

$$\theta_k = 12\eta^*\left\{\frac{\theta_kq_0 + \theta_{k-1}q_1}{2}\delta + \frac{\theta_{k-1}q_1 + \theta_{k-2}q_2}{2}\delta \right.$$

$$\left. + \ldots + \frac{\theta_{k-N+1}q_{N-1} + \theta_{K-N}q_N}{2}\delta\right\}. \tag{9}$$

Note $q'_N = 0$. Solving Eq. (9) for θ_k noting $q_N = 0$, then

$$\begin{cases} \theta_k = -k\delta, & \text{for} \quad k < N \\ \theta_k = \dfrac{12\eta^*\delta}{1 - 6\eta^*q_0\delta}\displaystyle\sum_{j=1}^{N-1}\theta_{k-j}q_j, & \text{for} \quad k \geq N. \end{cases} \tag{10}$$

After calculating θ_k from expression (10), the radial distribution function, g_k, is obtained by

$$\begin{cases} g_k = 0, & \text{for} \quad k < N(x^* < 1) \\ g_k = \dfrac{\theta_k}{k\delta} + 1, & \text{for} \quad k \geq N(x^* \geq 1). \end{cases} \tag{11}$$

A calculated example of $g(x^*)$ is shown in Fig. 4 (where $N = 100$, $\rho^*\sigma^3 = 0.8$). It is found that $g(x^*)$ oscillates when x^* is small, and steeply converges to 1 with the increase in x^*, which are generally well-known characteristics of the radial distribution function.

This is Perram's method (stepwise method) for solving the (transformed) Ornstein-Zernike equation.

3.3 Calculation of Solvation Pressure in Two-Phase System. In order to calculate the solvation pressure in long range by using the Derjaguin approximation, we should consider a two-phase system shown in Fig. 5 in which two large particles (diameter σ_1) are immersed in many small particles (diameter σ_2) and then we can calculate the interaction pressure between the two large particles. In the following theory, suffix 1 and 2 represent large and small particles, respectively.

The Ornstein-Zernike equation in a two-phase system as shown in Fig. 5 is written (Baxter, 1970)

$$h^*_{i,j}(r) = c^*_{i,j}(r) + \sum_{k=1}^{2}\rho^*_k\int c^*_{i,k}(s)h^*_{k,j}(|r - s|)ds, \tag{12}$$

where i, j are 1 or 2 and $h^*_{i,j}$ is indirect correlation function between particles i and j. Note that $h^*_{i,j} = h^*_{j,i}$ $(i \neq j)$ due to their symmetry (Baxter, 1970). The transformed Ornstein-Zernike equation is (Baxter, 1970)

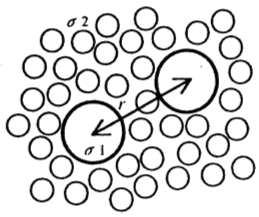

Fig. 5 Two-phase system. The system is composed of two kinds of particles; two large particles (diameter σ_1) and many small particles (diameter σ_2).

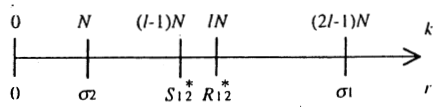

Fig. 6 Coordinate system

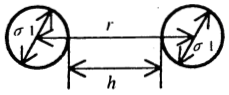

Fig. 7 Center separation, r, and surface separation, h

$$rh^*_{i,j}(r) = -q'_{i,j}(r) + 2\pi \sum_{k=1}^{2} \rho^*_k \times \int_{S^*_{i,k}}^{R^*_{i,k}} (r-t)h^*_{k,j}(|r-t|)q_{i,k}(t)dt, \quad (13)$$

where

$$\begin{cases} R^*_{i,j} = \dfrac{\sigma_i + \sigma_j}{2} \\ S^*_{i,j} = \dfrac{\sigma_i - \sigma_j}{2} \\ q'_{i,j}(r) = 0, \quad \text{for} \quad r > R^*_{i,j} \\ q'_{i,j}(r) = a_i r + b_j, \quad \text{for} \quad r \le R^*_{i,j} \\ q_{i,j}(r) = 0, \quad \text{for} \quad r > R^*_{i,j} \\ q_{i,j}(r) = \dfrac{1}{2}a_i(r^2 - R^{*2}_{i,j}) + b_i(r - R^*_{i,j}), \quad \text{for} \quad r \le R^*_{i,j} \\ a_i = \dfrac{1 - \xi_3 + 3\sigma_i\xi_2}{(1-\xi_3)^2} \\ b_i = \dfrac{-3\sigma_i^2\xi_2}{2(1-\xi_3)^2} \\ \xi_i = \dfrac{\pi}{6}\sum_{j=1}^{2}\rho^*_j\sigma^i_j \end{cases} \quad (14)$$

$h^*_{i,j}$ are calculated by Perram's method. As shown in Fig. 6, we set $\sigma_1 = (2l-1)\sigma_2$ (l: integer) and divide σ_2 into $(N+1)$ calculation points, i.e., $0, \delta, 2\delta, \ldots, N\delta = \sigma_2$ at which $q_{i,j}[k] = q_{i,j}(k\delta)$, $\theta_{i,j}[k] = k\delta h_{i,j}(k\delta)$, and $g_{i,j}[k] = g_{i,j}(k\delta)$. Then Eq. (13) gives

$$\begin{cases} \theta_{1,1}[k] = -k\delta, \quad \text{for} \quad 0 \le k < (2l-1)N \\ \theta_{1,1}[k] = \{\pi\rho^*_2\delta\theta_{1,2}[k-(l-1)N]q_{1,2}[(l-1)N] \\ \quad + 2\pi\rho^*_2\delta\sum_{j=1}^{lN-1}\theta_{1,2}[k-j]q_{1,2}[j] + 2\pi\rho^*_1\delta \\ \quad \times \sum_{j=1}^{(2l-1)N-1}\theta_{1,1}[k-j]q_{1,1}[j]\}/\{1 - \pi\rho^*_1\delta q_{1,1}[0]\}, \\ \qquad\qquad \text{for} \quad (2l-1)N \le k \end{cases} \quad (15)$$

$$\begin{cases} \theta_{1,2}[k] = -k\delta, \quad \text{for} \quad 0 \le k < lN \\ \theta_{1,2}[k] = \{\pi\rho^*_2\delta\theta_{2,2}[k-(l-1)N]q_{1,2}[(l-1)N] \\ \quad + 2\pi\rho^*_2\delta\sum_{j=1}^{lN-1}\theta_{2,2}[k-j]q_{1,2}[j] \\ \quad + \pi\rho^*_1\delta\theta_{1,2}[k-lN]q_{1,1}[lN] + 2\pi\rho^*_1\delta \\ \quad \times \sum_{j=1}^{lN-1}\theta_{1,2}[k-j]q_{1,1}[j]\}/\{1 - \pi\rho^*_1\delta q_{1,1}[0]\}, \\ \qquad\qquad \text{for} \quad lN \le k \end{cases} \quad (16)$$

$$\begin{cases} \theta_{2,2}[k] = -k\delta, \quad \text{for} \quad 0 \le k < N \\ \theta_{2,2}[k] = \{\pi\rho^*_1\delta\theta_{1,2}[k]q_{2,1}[0] + 2\pi\rho^*_1\delta \\ \quad \times \sum_{j=1}^{lN-1}\theta_{1,2}[|k-j|]q_{2,1}[j]f(k,j) + 2\pi\rho^*_2\delta \\ \quad \times \sum_{j=1}^{N-1}\theta_{2,2}[k-j]q_{2,2}[j]\}/\{1 - \pi\rho^*_2\delta q_{2,2}[0]\}, \\ \qquad\qquad \text{for} \quad N \le k \end{cases} \quad (17)$$

where

$$\begin{cases} f(k,j) = 1, & \text{for} \quad j \le k \\ f(k,j) = -1, & \text{for} \quad j > k \end{cases} \quad (18)$$

From expressions (15)–(17), the radial distribution function is

$$\begin{cases} g_{i,j}[k] = 0, & \text{for} \quad k = 0 \\ g_{i,j}[k] = \dfrac{\theta_{i,j}[k]}{k\delta} + 1, & \text{for} \quad k \ge 1 \end{cases} \quad (19)$$

Performing the central difference for expression (5) and substituting expression (19), then we get

$$F^{p-p}_{i,j}[k] = -\frac{k_BT}{2\pi R^{\text{eff}}_{i,j}\delta^2}\{g_{i,j}[k+1] - 2g_{i,j}[k] + g_{i,j}[k-1]\}. \quad (20)$$

Expression (20) gives solvation pressure between particles i and j. We should now remember that the Derjaguin approximation cannot be applied unless radii of interacting particles are much larger than surface separation. Considering this limitation, the solvation pressures regarding small particles ($F^{p-p}_{1,2}$ and $F^{p-p}_{2,2}$) are meaningless, although we can calculate them from expression (20). We need only $F^{p-p}_{1,1}$ because $F^{p-p}_{1,1}$ is the solvation force which acts between planes per unit area, i.e., p_s, when small particles intervene between the planes. We should note that ex-

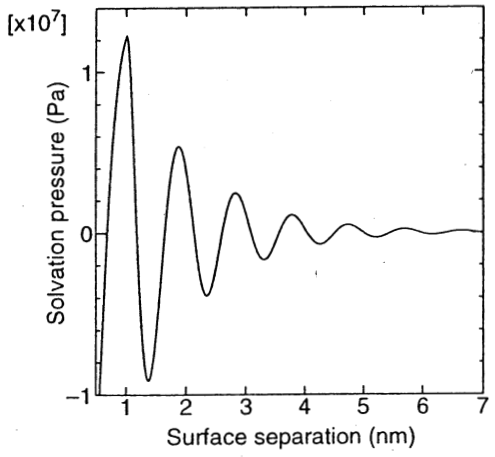

Fig. 8 Solvation pressure calculated by present method. $\rho^*_1 = 2\ \text{m}^{-3}$, $l = 150$, $N = 100$, $\rho^*_2\sigma^3_2 = 0.8$, $\sigma_2 = 1$ nm.

pression (20) is with respect to the distance, r, between centers of two particles. In order to calculate the solvation pressure as a function of surface separation, h, as shown in Fig. 7, we should use the following expression instead of expression (20).

$$\begin{cases} p_s[i] = -\dfrac{2k_BT}{\pi\sigma_1\delta^2}\left\{\dfrac{\theta_{1,1}[(2l-1)N+i+2]}{((2l-1)N+i+2)\delta}\right. \\ \left. -\dfrac{2\theta_{1,1}[(2l-1)N+i+1]}{((2l-1)N+i+1)\delta}+\dfrac{\theta_{1,1}[(2l-1)N+i]}{((2l-1)N+i)\delta}\right\}, \\ \text{for} \quad h[i]=(i+1)\delta \quad \text{and} \quad i \geq 1 \end{cases} \tag{21}$$

where $F_{1,1}^{p-p}$ is renamed p_s, and the effective radius of curvature of surfaces, R^{eff}, is given by (White, 1983; Israelachvili, 1992)

$$R_{i,j}^{\text{eff}} = \frac{\sigma_i\sigma_j}{2(\sigma_i+\sigma_j)} \tag{22}$$

We should note the values of ρ_1^*, $\rho_2^*\sigma_2^3$, l and N when we calculate the solvation pressure from these expressions. First, it is known that $\rho_2^*\sigma_2^3$ is about $0.7 \sim 0.9$ for almost all liquids (van Megen and Snook, 1979; Snook and van Megen, 1979; Heyes et al., 1980). Then the authors adopted $\rho_1^* = 2$ m^{-3} because we consider two large particles. By the investigation of convergence of the solvation pressure by changing l and N, it was found that converged value was obtained for $l \geq 100$ and $N \geq 75$. As a result, the authors adopted $\rho_1^* = 2$ m^{-3}, $l = 150$ ($\sigma_1 = 299\ \sigma_2$), $N = 100$ and $\rho_2^*\sigma_2^3 = 0.8$. An example of calculated solvation pressure is shown in Fig. 8 ($\sigma_2 = 1$ nm).

4 van der Waals Pressure

It is known that the van der Waals force acts between two surfaces (Lifshitz, 1956) when they are separated by a very thin liquid as shown in Fig. 9, in which surfaces are denoted by 1 and the liquid is by 3. The van der Waals pressure, p_{vdW} is given by (Israelachvili, 1972, 1992; Prieve and Russel, 1988)

$$p_{vdW} = -\frac{dW_{vdW}}{dh}, \quad W_{vdW} = -\frac{A_{131}}{12\pi h^2}, \tag{23}$$

$$\begin{cases} A_{131} = -\dfrac{3}{2}k_BT\sum_{n=0}^{\infty}{}'\int_{r_n}^{\infty} x\{\ln(1-\Delta_{13}^2e^{-x})+\ln(1-\bar{\Delta}_{13}^2e^{-x})\}dx \\ \Delta_{jk} = \dfrac{\epsilon_j s_k - \epsilon_k s_j}{\epsilon_j s_k + \epsilon_k s_j}, \quad \bar{\Delta}_{jk} = \dfrac{s_k - s_j}{s_k + s_j}, \quad s_k^2 = x^2 + \left(\dfrac{2\xi_n h}{c}\right)^2(\epsilon_k - \epsilon_3) \\ r_n = \dfrac{2h\xi_n\sqrt{\epsilon_3}}{c}, \quad \xi_n = \dfrac{2\pi n k_BT}{\hbar}, \quad \epsilon_j = \epsilon_k(i\xi_n), \quad \hbar = \dfrac{h_p}{2\pi} \\ \epsilon_k(i\xi_n) = \begin{cases} 1+\dfrac{n_k^2-1}{1+\xi_n^2/\omega_k^2} & (\text{for } \xi_n > 0), \\ \epsilon_{k0} & (\text{for } \xi_n = 0) \end{cases} \end{cases} \tag{24}$$

where h is surface separation, c is the speed of light, h_p is the Plank constant, n_k is refractive index, ω_k is absorption frequency and ϵ_{k0} is dielectric constant.

5 Hydrodynamic Viscous Pressure

In this study, we perform the EHL calculation for circular contacts between a sphere and a plane. The hydrodynamic viscous pressure, p_h, can be obtained by solving the following Reynolds equation

$$\frac{\partial}{\partial X}\left(\frac{\bar{\rho}H^3}{\bar{\eta}}\frac{\partial P_h}{\partial X}\right)+\frac{\partial}{\partial Y}\left(\frac{\bar{\rho}H^3}{\bar{\eta}}\frac{\partial P_h}{\partial Y}\right) = 12U\frac{a}{R}\frac{\partial(\bar{\rho}H)}{\partial X}, \tag{25}$$

$$\begin{cases} X = \dfrac{x}{a}, \quad Y = \dfrac{y}{a}, \quad \bar{\rho} = \dfrac{\rho}{\rho_0}, \bar{\eta} = \dfrac{\eta}{\eta_0}, \\ H = \dfrac{h}{R}, \quad P_h = \dfrac{p_h}{E'}, \quad U = \dfrac{\eta_0 u}{2RE'}, \\ a = \left(\dfrac{3R_eF}{E'}\right)^{1/3}, \quad E' = \dfrac{E}{1-\nu^2}, \quad R_e = \dfrac{R}{2} \end{cases} \tag{26}$$

where F is normal load (let us call it "fluid force"), E is Young's modulus, ν is Poisson's ratio, R is radius of curvature of the sphere, ρ_0 is density at ambient pressure, η_0 is viscosity at ambient pressure and a is the Hertzian radius of contact circle. The authors use the following expressions for pressure-density and pressure-viscosity relations (Dowson and Higginson, 1977; Hamrock and Dowson, 1976; Roelands et al., 1963),

$$\begin{cases} \bar{\rho} = \dfrac{\rho}{\rho_0} = 1 + \dfrac{\rho_1 P_h E'}{1+\rho_2 P_h E'}, \quad \rho_1 = 0.58, \quad \rho_2 = 1.68 \\ \bar{\eta} = \dfrac{\eta}{\eta_0} = \exp\left[(\ln\eta_0+\eta_1)\left\{\left(1+\dfrac{P_hE'}{\eta_2}\right)^Z - 1\right\}\right] \\ Z = \dfrac{\eta_1\alpha}{\ln\eta_0+\eta_1}, \quad \eta_1 = 9.67, \quad \eta_2 = 1.9609\times10^8\ (\text{Pa}) \end{cases} \tag{27}$$

where α is the pressure-viscosity coefficient and the authors assumed that $\alpha = 10$ GPa^{-1}. Now we have presented all pressure components in expression (1), namely, p_s, p_{vdW} and p_h.

6 Elasticity Equation

The film thickness is given by (Evans and Snidle, 1981)

$$H(X,Y) = H_0 + \frac{S(X,Y)}{R} + \frac{w(X,Y)}{R} - \frac{w_0}{R}, \tag{28}$$

where H is the dimensionless film thickness, H_0 is film thickness at the center of Hertzian contact, S is separation due to the

geometry of the spherical solid, w is elastic deformation and w_0 is elastic deformation at the center of Hertzian contact. When the total pressure, p, in expression (1) is obtained, the elastic deformation of solid is given by (Hamrock and Dowson, 1976)

$$w(X, Y) = \frac{2a}{\pi} \int_{-\infty}^{\infty} \int_{-\infty}^{\infty} \frac{P(X', Y')dX'dY'}{\sqrt{(X - X')^2 + (Y - Y')^2}} \quad (29)$$

where P is dimensionless pressure, $P = p/E'$.

In conventional EHL calculations, Eq. (25) and expression (29) are solved simultaneously. There are several methods proposed in past studies to solve EHL problems (Hamrock and Dowson, 1976; Evans and Snidle, 1981; Lin and Chu, 1991, Venner and ten Napel, 1992(a), (b)), and the authors adopt the ϕ-solution proposed by Hamrock and Dowson (1976). Formulations of (25) and (29), boundary condition and initial condition are described in detail by Hamrock and Dowson (1976). The number of grid points per dimensionless unit length (normalized by Hertzian contact radius, a) is 10 both in X, Y directions (Chittenden et al., 1985), and the criteria of convergence in relaxation method are same as Jang and Tichy (1995). The calculation for not only the elastohydrodynamic regime but also the hydrodynamic regime was performed. The authors take a large calculation region, i.e., $-\gamma \le X \le 3$, $-\gamma \le Y \le \gamma$, where $\gamma = 50 \sim 70$. The calculation of elastic deformation takes so much calculation time that the authors assumed that the elastic deformed region is $-3 \le X \le 3$, $-3 \le Y \le 3$. The programing language which the authors used is the C language on a UNIX machine (HP Apollo Series 735). The van der Waals pressure and the solvation pressure for surface separation, h, are calculated beforehand and saved in data files, and the two pressures are calculated by linear interpolation for obtained h at each grid point. The authors have confirmed that the numerical results considering only the hydrodynamic viscous pressure and setting the van der Waals pressure and the solvation pressure to be zero give a good agreement with past calculations (Hamrock and Dowson, 1978). The flowchart of the program is not described here since its detail is almost the same as in past studies (Hamrock and Dowson, 1976; Evans and Snidle, 1981; Lin and Chu, 1991; Venner and ten Napel, 1992(a), (b); Chittenden et al., 1985).

7 Experimental Outline

The authors developed a new apparatus which can measure film thickness accurately between two cylinder surfaces with curvature radius R of about 10 mm in a crossed configuration, which is geometrically equivalent to the configuration between a sphere and a plane (Israelachvili, 1992). In the authors' experiments, mica was used as a solid specimen, and octamethylcyclotetrasiloxane (OMCTS), cyclohexane and n-hexadecane were used as liquid specimens. Properties of these specimens which are required for the present calculation are listed in Table 1 and 2. The sliding speed of the two surface is 200 μm/s. The apparatus and experimental procedure are described in detail elsewhere (Matsuoka and Kato, 1996).

8 Other Solvation Pressure Models

8.1 Jang and Tichy's Model. Jang and Tichy (1995) proposed the following exp-cos model for solvation pressure

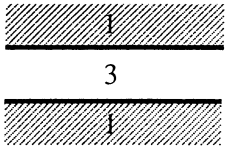

Fig. 9 van der Waals interaction between planes

Table 1 Properties of Mica

chemical formula	$K(Al_2)(Si_3Al)O_{10}(OH)_2$[a]
refractive index n	1.60[b]
absorption frequency ω	1.9×10^{16} rad/s[b]
dielectric constant ϵ_0	7.0[c]
Young's modulus E	34.5 GPa*
Poisson's ratio ν	0.205*

a: (Gains, 1957), b: (Horn and Israelachvili, 1981), c: (Israelachvili, 1992), * denotes measured value.

on the analogy of characteristics of the solvation force referring Chan and Horn's report (1985),

$$p_s = -C_s \exp\left(-\frac{h}{\sigma}\right) \cos\left(\frac{2\pi h}{\sigma}\right), \quad (30)$$

where p_s is the solvation pressure, C_s is a constant, h is surface separation (we call it the film thickness) and σ is the molecular diameter of intervening liquid and $\sigma = 1$ nm with respect to octamethylcyclotetrasiloxane (OMCTS) (Israelachvili, 1992).

Jang and Tichy assumed that $C_s = 172$ MPa on the analogy of Chan and Horn's report in which OMCTS was used as intervening liquid between solid surfaces.

8.2 Chan and Horn's Model. Chan and Horn (1985) performed experiments of solvation force measurements in mica-liquid-mica system in which the solid surfaces (mica surfaces) were arranged in crossed cylinder configuration which is geometrically equivalent to plane-sphere configuration (White, 1983), and they proposed the following exp-cos model for net solvation force,

$$F_s^{s-p} = -RC_F \exp\left(-\frac{h}{\sigma}\right) \cos\left(\frac{2\pi h}{\sigma}\right), \quad (31)$$

where F_s is the net solvation force, superscript s-p denotes interaction between a $s$phere and a $p$lane, R is the radius of curvature of interacting solid surface and C_F is an unknown constant. They obtained the value of C_F by applying the least-square fitting of expression (31) to their experimental data where OMCTS was used and C_F was obtained as 172 mN/m. We should note that expression (31) is not a solvation pressure but a net solvation force between a sphere and a plane.

The Derjaguin approximation (4) is used to convert a net force between a sphere and a plane into a force between planes per unit area, namely, pressure. It is found that R^{eff} in expression (4) is equal to R (radius of curvature of the cylinder surface) in Chan and Horn's case. Applying the Derjaguin approximation to expression (31),

$$W^{p-p} = -\frac{C_F}{2\pi} \exp\left(-\frac{h}{\sigma}\right) \cos\left(\frac{2\pi h}{\sigma}\right) \quad (32)$$

and solvation pressure, p_s, is given by

$$p_s = F^{p\text{-}p} = -\frac{dW^{p\text{-}p}}{dh} = -\frac{\sqrt{1 + 4\pi^2}C_F}{2\pi\sigma} \exp\left(-\frac{h}{\sigma}\right) \times \cos\left(\frac{2\pi h}{\sigma} + \varphi\right), \quad \tan\varphi = -2\pi. \quad (33)$$

Coefficient of expression (33) is 174 MPa from $C_F = 172$ mN/m. It is seen from expressions (30) and (33) that the difference between two models is only in the phase factor, φ, because the coefficients are almost same. Expression (30) or (33) are substituted into expression (1) and EHL problem is solved by the same method as stated in Section 6.

Table 2 Properties of liquids

Liquid	OMCTS	Cyclohexane	*n*-hexadecane
chemical formula	$[(CH_3)_2SiO]_4$[d]	$(CH_2)_6$[e]	$CH_3(CH_2)_{14}CH_3$[f]
diameter σ	1 nm[d]	0.6 nm[e]	0.4 nm[f]
refractive index n	1.40[d]	1.43[e]	1.42[f]
absorption frequency ω	1.60×10^{16} rad/s[d]	1.82×10^{16} rad/s[f]	1.82×10^{16} rad/s[f]
dielectric constant ϵ_0	2.30[d]	2.02[e]	2.05[f]
viscosity η_0	2.35 mPa·s[d]	0.980 mPa·s[e]	3.35 mPa·s[f]

d: (Horn and Israelachvili, 1981), e: (Christenson, 1983), f: (Israelachvili, 1992).

It should be noted that since the solvation pressure depends on the molecular structure of liquid, we can apply the two models described in the Subsection 8.1 and 8.2 with the values of coefficients (C_F or C_s) only to the case where OMCTS is used.

9 Results and Discussion

9.1 Comparison of the Present Model With Experiments. Figure 10 shows an example of calculated pressure distribution by using the present solvation pressure model for OMCTS. It is found that the oscillatory solvation force lies on the conventional hydrodynamic viscous pressure. If the film thickness is smaller than this example the viscous pressure becomes negligible and the solvation pressure becomes dominant. According to Hamrock-Dowson diagram (Esfahanian and Hamrock, 1991) the sliding condition of this example falls into Rigid-Isoviscous region where elastic surface deformation is negligible. The surface deformation due to the solvation pressure was also small and noted EHL film shape, namely the flattened center and the occurrence of minimum film thickness at the trailing edge, was not obtained under this sliding condition. Figure 11 shows the relation between the fluid force, F, and the film thickness, h, which is obtained by summarizing raw data like Fig. 10. Black dots represent experimental results, the thin solid line is the conventional theoretical line in R-I regime (Venner and ten Napel, 1992(b)), the thin dashed line and thin dot-dashed line are theoretical minimum and central film thickness in E-I regime (Hamrock and Dowson, 1978), respectively, and the thick solid line shows results of EHL calculation by using the present solvation pressure model for OMCTS. The solvation pressure is calculated assuming $\sigma_2 = 1$ nm (see Table 2). It is seen in Fig. 11 that the film thickness begins to deviate from the conventional EHL theory when the film thickness is less than about 7 ~ 8 nm and changes stepwise. The present model gives good agreement with the experiments on the whole though it overestimates the fluid force slightly when the film thickness is about 1 ~ 2 nm. An advantage of the present calculation is that laborious and difficult experiments are not required in order to obtain unknown parameters (Chan and Horn, 1985; Tichy, 1995(a), (b), (c); Jang and Tichy, 1995).

Figure 12 shows a comparison of experimental results with calculation results obtained by the present method for cyclohexane. The discretization of film thickness is again observed as in the OMCTS results, and the interval is 0.5 ~ 0.6 nm, which is roughly same as the molecular diameter of cyclohexane (see Table 2). The solvation pressure is calculated assuming σ_2 = 0.6 nm (see Table 2). The present calculation agrees well with the experimental data also in the case of cyclohexane.

It is considered that the present calculation agrees well with the experiments for the liquids which have strong solvation force such as OMCTS and cyclohexane (Horn and Israelachvili, 1981; Christenson et al., 1982). The authors performed experiments for *n*-hexadecane, which shows very little solvation force (Christenson et al., 1982; Gee et al., 1990) and compared it with the theory. They are shown in Fig. 13 in which the solvation pressure is calculated assuming σ_2 = 0.4 nm (see Table 2). The discretization of the film thickness is not observed from the experiments in this case, and the calculation result does not agree with the experimental results. This may be because long chain molecules of *n*-hexadecane have flexibility, are entangled in each other in the vicinity of solid surface, and therefore, *n*-hexadecane shows very little solvation force (Christenson et al., 1982; Gee et al., 1990). It may be difficult to apply the present theory to liquids that have a molecular shape far from spherical and exhibit weak solvation force.

It is noted that calculation time to obtain Fig. 11–13 was 10 ~ 15 days, respectively.

9.2 Comparison of Solvation Pressure Models. Now we compare the three solvation pressures. Fig. 14 shows the solvation pressures for OMCTS. It is found that oscillation am-

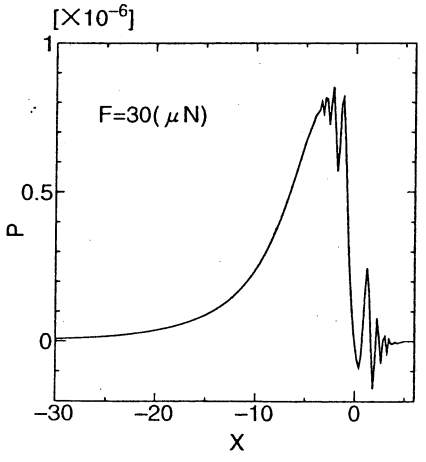

Fig. 10 An example of pressure distribution by the present EHL calculation, showing oscillatory pressure distribution due to the solvation pressure

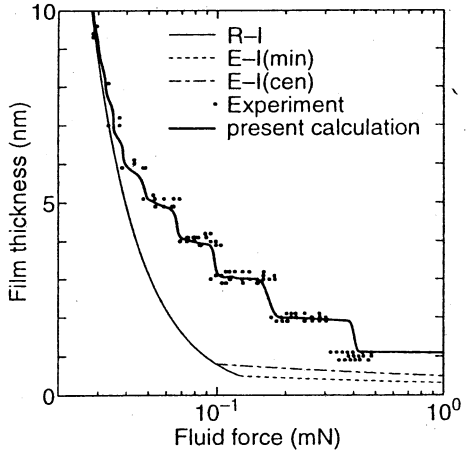

Fig. 11 EHL calculation result for OMCTS

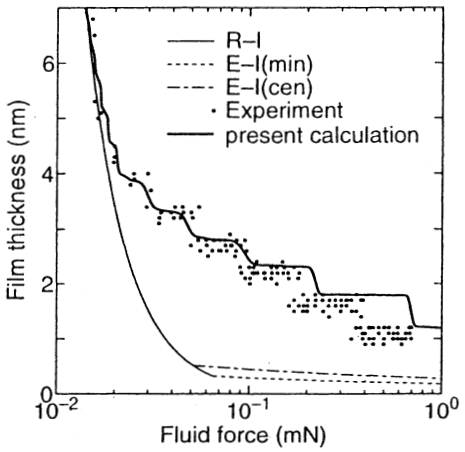

Fig. 12 EHL calculation result for cyclohexane

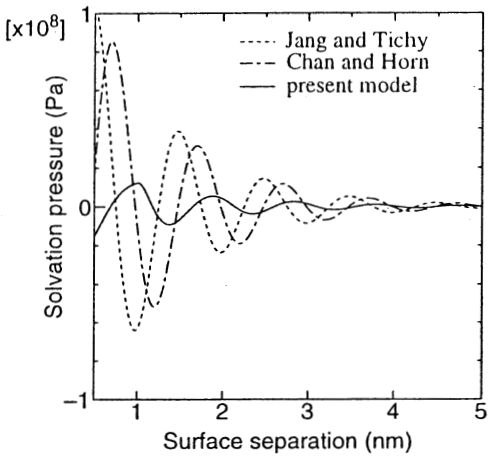

Fig. 14 Solvation pressures for OMCTS, showing three solvation pressure models

plitudes by Jang and Tichy's model and by Chan and Horn's model are remarkably larger than the present model.

Let us consider why Jang and Tichy's and Chan and Horn's solvation pressure is much larger than the present calculation. Chan and Horn obtain the coefficients, C_F, in expression (31) from experimental results using crossed cylinder surfaces by supposing that the surfaces are rigid bodies and elastic deformation of the solid surfaces is neglected. However, when we look at Fig. 15 which shows a calculation result of elastic deformation of the mica surface only by the solvation pressure obtained by the present model, it is seen that flattened deformation of solid surface due to the solvation pressure cannot be neglected any more. Note that the calculation conditions are $H = h/R$, $R = 10$ mm, $P = p_s/E'$, $E' = 36.0$ GPa, $X = x/a$ and $a = 4.71 \times 10^{-6}$ m. Since this elastic deformation makes the surfaces approach closer, the deformation produces much larger solvation force in experimental, macroscopic observations. In other words, if the elastic deformation is neglected, the solvation pressure is overestimated. Hence, the elastic deformation should not be neglected even when the solvation pressure is approximated by the exp-cos type model like expressions (30) and (33). It is considered that the phase deviation among the models is also caused by the elastic deformation.

Finally, the results of present calculation and two other models are compared in Fig. 16 with the experimental results of the film thickness for OMCTS. Elastic deformation is considered in all models. It is seen that although the Jang and Tichy's model shows the stepwise decrease in the film thickness it predicts larger film thickness than the experimental results and the agreement of the phase of the stepwise change of the film thickness with the experiments is poor. The stepwise change of the film thickness is not found in the original Jang and Tichy's calculation (1995). This may be because (i) the viscous pressure is so large under the condition of their calculation that the solvation pressure hardly affects the film thickness change and (ii) there is not a sufficient number of calculations to obtain the stepwise film thickness change in their report. When we look at the results of Chan and Horn's model, it is seen that the phase agrees well with the experiments, but the predicted film thickness is again very larger compared with the experiments. It is noted, thus, that the elastic deformation of the solid surface should be taken into account for obtaining the parameter of exp-cos model when the film thickness is so small that the solvation force cannot be neglected.

10 Conclusions

The authors developed a new method for the calculation of solvation pressure in which the transformed Ornstein-Zernike equation for hard-spheres in a two-phase system was solved by Perram's method (stepwise method) and the Derjaguin approximation was used. The present theory does not include experimental parameters. The authors applied the solvation pressures to the EHL calculation and compared the calculation results with experimental data. It was found that the present calculation agrees well with the experimental data.

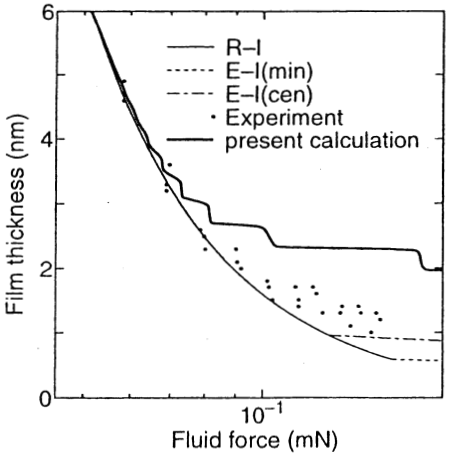

Fig. 13 EHL calculation result for *n*-hexadecane

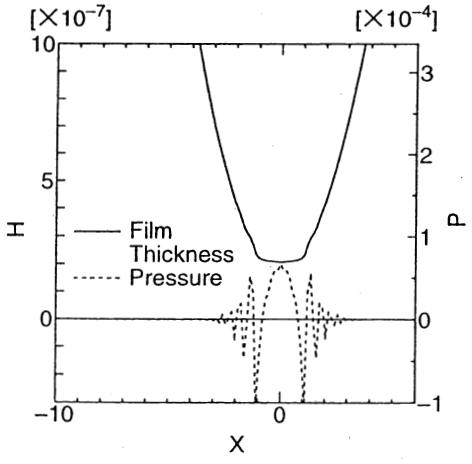

Fig. 15 A calculation result of elastic deformation of mica surface due to solvation pressure of OMCTS. The solvation pressure is calculated by the present model.

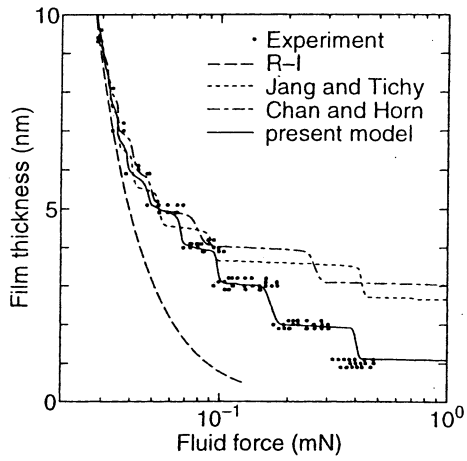

Fig. 16 Comparison of three solvation pressure models with the experiments for OMCTS

In order to ensure the possibility of surface elastic deformation, film thickness was calculated using two conventional calculation models proposed so far in which the solvation force was considered but the surface elastic deformation was not assumed. It was found that these models overestimated the solvation pressure resulting in the larger film thickness.

Acknowledgment

The authors wish to thank Dr. M. Stanley at the Department of Mechanical Engineering, The University of Tokyo for helpful comments.

References

Alder, B. J., Frankel, S. P., Lewinson, V. A., 1955, "Radial Distribution Function Calculated by the Monte-Carlo Method for a Hard Sphere Fluid," *Journal of Chemical Physics,* Vol. 23, pp. 417–419.

Baxter, R. J., 1970, "Ornstein-Zernike Relation and Percus-Yevick Approximation for Fluid Mixtures," *Journal of Chemical Physics,* Vol. 52, pp. 4559–4562.

Bitsanis, I., Magda, J. J., Trrell, M., and Davis, H. T., 1987, "Molecular Dynamics of Flow in Micropores," *Journal of Chemical Physics,* Vol. 87, pp. 1733–1750.

Carson, G., Hu, H.-W., and Granick, S., 1992, "Molecular Tribology of Fluid Lubrication: Shear Thinning," STLE *Tribology Transactions,* Vol. 35, pp. 405–410.

Chan, D. Y. C., and Horn, R. G., 1985, "The Drainage of Thin Liquid Films between Solid Surfaces," *Journal of Chemical Physics,* Vol. 83, pp. 5311–5324.

Chittenden, R. J., Dowson, D., Dunn, J. F., and Taylor, C. M., 1985, "A Theoretical Analysis if the Isothermal Elastohydrodynamic Lubrication of Concentrated Contacts I. Direction of Lubricant Entrainment Coincident with the Major Axis of the Hertzian Contact Ellipse," *Proceedings of the Royal Society of London,* Series A, Vol. 397, pp. 245–269.

Christenson, H. K., 1983, "Experimental Measurements of Solvation Forces in Nonpolar Liquids," *Journal of Chemical Physics,* Vol. 78, pp. 6906–6913.

Christenson, H. K., Horn, R. G., and Israelachvili, J. N., 1982, "Measurement of Forces Due to Structure in Hydrocarbon Liquids," *Journal of Colloid and Interface Science,* Vol. 88, pp. 79–88.

de Bruyne, F. A., and Bogy, D. B., 1994, "Numerical Simulation of the Lubrication of the Head-Disk Interface Using a Non-Newtonian Fluid," ASME JOURNAL OF TRIBOLOGY, Vol. 116, pp. 541–548.

Dowson, D., and Higginson, G. R., 1977, "Elasto-Hydrodynamic Lubrication," SI edition, Pergamon Press.

Esfahanian, M., and Hamrock, B. J., 1991, "Fluid-Film Lubrication Regimes Revisited," STLE *Tribology Transactions,* Vol. 34, pp. 628–632.

Evans, H. P., and Snidle, R. W., 1981, "The Isothermal Elastohydrodynamic Lubrication of Spheres," ASME JOURNAL OF LUBRICATION TECHNOLOGY, Vol. 103, pp. 547–557.

Gaines, Jr., G. L., 1957, "The Ion-Exchange Properties of Muscovite Mica," *Journal of Physical Chemistry,* Vol. 61, pp. 1408–1413.

Gee, M. L., McGuiggan, P. M., Israelachvili, J. N., and Homola, A. M., 1990, "Liquid to Solidlike Transition of Molecularly Thin Films under Shear," *Journal of Chemical Physics,* Vol. 93, pp. 1895–1906.

Georges, J. M., Millot, S., Loubet, J. L., and Tonk, A., 1993(a), "Drainage of Thin Liquid Films between Relatively Smooth Surfaces," *Journal of Chemical Physics,* Vol. 98, pp. 7345–7360.

Georges, J. M., Millot, S., Loubet, J. L., Tonk, A., and Mazuyer, D., 1993(b), "Surface Roughness and Squeezed Films at Molecular Level," *Proceedings of the 19th Leeds-Lyon Symposium on Tribology,* pp. 443–452.

Georges, J. M., Tonk, A., Mazuyer, D., 1995, "Static and Dynamic Frictions of Compressed Polymer Layers," *Synopses of International Tribology Conference '95,* Yokohama, pp. 1.

Granick, S., 1991, "Motions and Relaxations of Confined Liquids," *Science,* Vol. 253, pp. 1374–1379.

Granick, S., and Hu, H.-W., 1994, "Nanorheology of Confined Polymer Melts. 1. Linear Shear Response at Strongly Adsorbing Surfaces," *Langmuir,* Vol. 10, pp. 3857–3866.

Granick, S., Demirel, A. L., Cai, L. L., and Peanasky, J., 1995, "Nanorheology of Confined Liquids and Block Copolymers," *Israel Journal of Chemistry,* Vol. 35, pp. 75–84.

Guangteng, G., and Spikes, H. A., 1994, "Behavior of Lubricants in the Mixed Elastohydrodynamic Regime," presented at the 21st Leeds-Lyon Symposium on Tribology.

Guangteng, G., and Spikes, H. A., 1995, "Boundary Film Formation by Lubricant Base Fluids," presented at the 50th STLE Annual Meeting in Chicago, No. 95-NP-7D-3.

Hamrock, B. J., and Dowson, D., 1976, "Isothermal Elastohydrodynamic Lubrication of Point Contacts Part 1—Theoretical Formulation," ASME JOURNAL OF LUBRICATION TECHNOLOGY, Vol. 98, pp. 223–229.

Hamrock, B. J., and Dowson, D., 1978, "Minimum Film Thickness in Elliptical Contacts for Different Regimes of Fluid Film Lubrication," *Proceedings of the 5th Leeds-Lyon Symposium on Tribology,* pp. 22–27.

Henderson, D., and Lozada-Cassou, M., 1986, "A Simple Theory for the Force between Spheres Immersed in a Fluid," *Journal of Colloid and Interface Science,* Vol. 114, pp. 180–183.

Heyes, D. M., Kim, J. J., Montrose, C. J., and Litovitz, T. A., 1980, "Time Dependent Nonlinear Shear Stress Effects in Simple Liquids: A Molecular Dynamics Study," *Journal of Chemical Physics,* Vol. 73, pp. 3987–3996.

Homola, A. M., 1991, "The Role of Interfacial Forces and Lubrication in Thin-Film Magnetic Media," *Advences in Information Storage System,* Vol. 1, pp. 279–308.

Homola, A. M., Israelachvili, J. N., Gee, M. L., and McGuiggan, P. M., 1989, "Measurement of and Relation between the Adhesion and Friction of Two Surfaces Separated by Molecularly Thin Liquid Films," ASME JOURNAL OF TRIBOLOGY, Vol. 111, pp. 675–682.

Horn, R. G., and Israelachvili, J. N., 1981, "Direct Measurement of Structural Forces between Two Surfaces in a Nonpolar Liquid," *Journal of Chemical Physics,* Vol. 75, pp. 1400–1411.

Ikeda, Y., and Tago, K., 1995, "Tribological Study on Molecularly Thin Films Using Non-Equilibrium Molecular Dynamics," *JAST Journal of Japanese Society of Tribologists,* Vol. 40, pp. 253–259.

Israelachvili, J. N., 1972, "The Calculation of van der Waals Dispersion Forces between Macroscopic Bodies," *Proceedings of the Royal Society of London,* Series A, Vol. 331, pp. 39–55.

Israelachvili, J. N., 1992, "Intermolecular and Surface Forces," 2nd edition, Academic Press.

Israelachvili, J. N., McGuiggan, P. M., and Homola, A. M., 1988, "Dynamic Properties of Molecularly Thin Liquid Films," *Science,* Vol. 240, pp. 189–191.

Jang, S., and Tichy, J. A., 1995, "Rheological Models for Thin Film EHL Contacts," ASME JOURNAL OF TRIBOLOGY, Vol. 117, pp. 22–28.

Johnston, G. J., Wayte, R., and Spikes, H. A., 1991, "The Measurement and Study of Very Thin Lubricant Films in Concentrated Contacts," STLE *Tribology Transactions,* Vol. 34, pp. 187–194.

Lifshitz, E. M., 1956, "The Theory of Molecular Attractive Forces between Solids," *Soviet Physics, JETP,* Vol. 2, pp. 73–83.

Lin, J. F., and Chu, H. Y., 1991, "A Numerical Solution for Calculating Elastic Deformation in Elliptical-Contact EHL of Rough Surface," ASME JOURNAL OF TRIBOLOGY, Vol. 113, pp. 12–21.

Luo, J. B., Wen, S. Z., and Cao, N. J., 1995, "Study on the Characteristics of Lubricant Film at Nanometer Scale," *Synopses of International Tribology Conference '95,* Yokohama, pp. 2.

Matsuoka, H., and Kato, T., 1996, "Discrete Nature of Ultrathin Lubrication Film Between Mica Surfaces," ASME JOURNAL OF TRIBOLOGY, to be published.

Ornstein, L. S., and Zernike, F., 1914, "Accidental Deviations of Density and Opalescence at the Critical Point of a Single Substance," *Proceedings of the Royal Academy,* Amsterdam, Vol. 17, pp. 793–806.

Peachey, J., van Alsten, J., and Granick, S., 1991, "Design of an Apparatus to Measure the Shear Response of Ultrathin Liquid Films," *Review in Scientific Instruments,* Vol. 62, pp. 463–473.

Percus, J. K., and Yevick, G. J., 1958, "Analysis of Classical Statistical Mechanics by Means of Collective Coordinates," *Physical Review,* Vol. 110, pp. 1–13.

Perram, J. W., 1975, "Hard Sphere Correlation Functions in the Percus-Yevick Approximation," *Molecular Physics,* Vol. 30, pp. 1505–1509.

Prieve, D. C., and Russel, W. B., 1988, "Simplified Predictions of Hamaker Constants from Lifshitz Theory," *Journal of Colloid and Interface Science,* Vol. 125, pp. 1–13.

Smeeth, M., Spikes, H. A., and Gunsel, S., 1995(a), "The Formation of Viscous Surface Films by Polymer Solutions: Boundary or Elastohydrodynamic Lubrication?," presented at the 50th STLE Annual Meeting in Chicago, No. 95-NP-7D-2.

Smeeth, M., Spikes, H. A., and Gunsel, S., 1995(b), "Boundary Film Formation by Viscosity Index Improvers," presented at the STLE/ASME Tribology Conference in Florida, No. 95-TC-3C-1.

Smith, W. R., and Henderson, D., 1970, "Analytical Representation of the Percus-Yevick Hard-Sphere Radial Distribution Function," *Molecular Physics,* Vol. 19, pp. 411–415.

Snook, I., and van Megen, W., 1979, "Structure of Dense Liquids at Solid Interfaces," *Journal of Chemical Physics,* Vol. 70, pp. 3099–3105.

Snook, I. K., and van Megen, W., 1980, "Solvation Forces in Simple Dense Fluids. I," *Journal of Chemical Physics,* Vol. 72, pp. 2907–2913.

Snook, I. K., and van Megen, W., 1981, "Calculation of Solvation Forces between Solid Particles Immersed in a Simple Liquid," *Journal of Chemical Society, Faraday Transactions II,* Vol. 77, pp. 181–190.

Spikes, H., 1995, "The Thickness and Rheology of Boundary Lubricating Films," Synopses of International Tribology Conference '95, Yokohama, pp. 3.

Tarazona, P., and Vicente, L., 1985, "A Model for Density Oscillations in Liquids between Solid Walls," *Molecular Physics,* Vol. 56, pp. 557–572.

Throop, G. J., and Bearman, R. J., 1965, "Numerical Solutions of the Percus-Yevick Equation for the Hard-Sphere Potential," *Journal of Chemical Physics,* Vol. 42, pp. 2408–2411.

Tichy, J. A., 1995(a), "Modeling of Thin Film Lubrication," *STLE Tribology Transactions,* Vol. 38, pp. 108–118.

Tichy, J. A., 1995(b), "A Surface Layer Model for Thin Film Lubrication," *STLE Tribology Transactions,* Vol. 38, pp. 577–582.

Tichy, J. A., 1995(c), "A Porous Media Model for Thin Film Lubrication," ASME JOURNAL OF TRIBOLOGY, Vol. 117, pp. 16–21.

van Alsten, J., and Granick, S., 1988, "Molecular Tribometry of Ultrathin Liquid Films," *Physical Review Letters,* Vol. 61, pp. 2570–2573.

van Alsten, J., and Granick, S., 1990, "Tribology Studied Using Atomically Smooth Surfaces," *STLE Tribology Transactions,* Vol. 33, pp. 436–446.

van Megen, W., and Snook, I., 1979, "Solvent Structure and Solvation Forces between Solid Bodies," *Journal of Chemical Society, Faraday Transactions II,* Vol. 75, pp. 1095–1102.

Venner, C. H., and ten Napel, W. E., 1992(a), "Multilevel Solution of the Elastohydrodynamically Lubricated Circular Contact Problem Part 1: Theory and Numerical Argorithm," *Wear,* Vol. 152, pp. 351–367.

Venner, C. H., and ten Napel, W. E., 1992(b), "Multilevel Solution of the Elastohydrodynamically Lubricated Circular Contact Problem Part 2: Smooth Surface Results," *Wear,* Vol. 152, pp. 369–381.

Wertheim, M. S., 1963, "Exact Solution of the Percus-Yevick Integral Equation for Hard Spheres," *Physical Review Letters,* Vol. 10, pp. 321–323.

Wertheim, M. S., 1964, "Analytic Solution of the Percus-Yevick Equation," *Journal of Mathematical Physics,* Vol. 5, pp. 643–651.

White, L. R., 1983, "On the Deryaguin Approximation for the Interaction of Macrobodies," *Journal of Colloid and Interface Science,* Vol. 95, pp. 286–288.